Deformable Object Behavior Reconstruction Derived Through Simultaneous Geometric and Material Property Estimation

Shane Transue(✉) and Min-Hyung Choi

University of Colorado Denver, Denver, USA
shane.transue@ucdenver.edu

Abstract. We present a methodology of accurately reconstructing the deformation and surface characteristics of a scanned 3D model recorded in real-time within a Finite Element Model (FEM) simulation. Based on a sequence of generated surface deformations defining a reference animation, we illustrate the ability to accurately replicate the deformation behavior of an object composed of an unknown homogeneous elastic material. We then formulate the procedural generation of the internal geometric structure and material parameterization required to achieve the recorded deformation behavior as a non-linear optimization problem. In this formulation the geometric distribution (quality) and density of tetrahedral components are simultaneously optimized with the elastic material parameters (Young's Modulus and Possion's ratio) of a procedurally generated FEM model to provide the optimal deformation behavior with respect to the recorded surface.

1 Introduction

Replicating realistic deformation behaviors of elastic objects is an extensively studied domain with a broad array of applications in countless fields including soft-tissue medicine, structural engineering, and animation. The ability to reliably reproduce physically plausible deformations exhibited by elastic objects has been widely developed and several techniques have been introduced in an effort to automate the process of reproducing realistic deformations of recorded real-world objects. Physically-based Finite Element Methods (FEM) define the standard for emulating realistic elastic behaviors demonstrated by deformable objects and provide accurate representations of physically plausible behaviors. While methods of estimating material properties, such as Young's modulus and Poisson's ratio for FEM-based physical models from scanned objects have been introduced [1,2], these techniques rely on the assignment of an arbitrary internal geometric structure contained by a scanned surface or use artistically created template meshes. The assumption that these techniques present is that the ideal material properties will accurately reproduce the observed deformation. The premise of our methodology deviates from this standard process through the introduction of a technique for simultaneously extracting both the ideal internal

G. Bebis et al. (Eds.): ISVC 2015, Part II, LNCS 9475, pp. 474–485, 2015.
DOI: 10.1007/978-3-319-27863-6_44

geometric density and homogeneous isotropic material properties to provide an accurate reconstruction of a recorded deformation.

In this work we present an automated extension of modeling physically simulated deformable objects and present a means to optimizing FEM-based physical models to behave consistently with their real-world counterparts. However, unlike most prior work within this field, we base our approach on the notion that strictly identifying the material parameters of a deformable object may not provide optimal behavioral correspondence to these real-world deformations. Typically the geometric composition of the simulated object has a large impact on the deformation behaviors that are exhibited by the object and can degrade the accuracy of the exhibited deformations. The images in Fig. 1 illustrate the impact of geometric density on the resulting deformation behavior of an FEM mesh with increasing geometric densities simulated using VegaFEM [3].

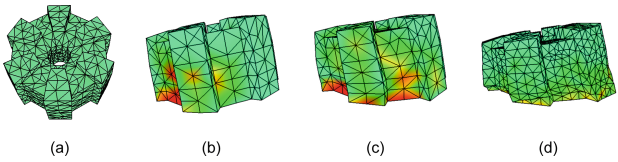

Fig. 1. Impact of the geometric density on an FEM for the deformation of a model (a) dropped onto a flat surface for resolutions of: (b) $n = 688$, (c) $n = 868$, and (d) $n = 4070$ nodes. Young's modulous (1.0e5) and Poisson's ratio (0.4) are held constant.

Based on this geometric density influence, we build upon existing methods for replicating an elastic-based deformation within a physical simulation, emphasizing the process of extracting the characteristics of the geometric density that facilitate the generation of the exhibited deformation. The objective of our approach is to procedurally generate both the geometric and material properties that provide the closest approximation of the deformation defined by the recorded surface. Additionally, our technique aims to provide a practical implementation that can automatically obtain the physical simulation template model and replicate the recorded deformation behavior without manual intervention.

2 Related Work

The extraction and estimation of the material properties of FEM-based objects has been extensively studied and several forms of material optimization techniques have been developed [4,5]. Multi-view tracking systems for iteratively reconstructing the deformation of an initial surface mesh have also been developed [6]. In relation to the methodology we present, independent aspects of our approach have been validated with respect to the optimization of deformable object animations. This includes the optimization of the underlying geometry of deformable mass-spring systems and associated material properties [7] and

the extraction of a physical surface model from a multi-view configuration [8]. Recently, template-based techniques have been developed [1] to eliminate the use of several scanning devices to improve the practicality of the scanning process; however our technique differs from this in that we continue to extract the simulation mesh (template) from the animated surface sequence (set of temporally coherent, aligned 3D scans) for our proposed optimization process.

Recent techniques propose an approach that utilizes a similar process for the extraction and optimization of the material parameters of the elastic material properties to match a provided input deformation [2]. In this work the observed deformation behavior is defined through signed distance fields that define the required deformation of the provided watertight surfaces. While the input to our method is consistent with this approach, our technique varies from this work in two aspects: (1) we continuously regenerate the rest-state internal geometry of the simulated FEM mesh to improve the consistency between the simulated surface and the provided animation and (2) the objective of our method is to provide a process for reconstructing the generalized deformation behavior without introducing undesirable secondary behaviors. These secondary behaviors can be introduced as surface artifacts within noisy surface scans and should not be incorporated within the reproduced deformation behavior.

3 Method

In the objective of reconstructing scanned deformation behaviors, we propose a methodology of capturing and emulating the deformations exhibited by a surface scanned by a set of high-speed depth-imaging devices. In this process we present an automated method of extracting the surface of the scanned object over time, the procedural generation of the tetrahedral simulation mesh, and the material coefficients used to recreate the observed deformation. We then optimize both the geometric and elastic material properties used to define the simulation mesh that provides the optimal approximation of the recoded deformation behavior.

The implemented method of reproducing the observed deformation behavior of the scanned surface model is based on a five-stage process: (1) The recorded deformation is provided as a set of surface scans (point-clouds) that defines the objects surface state at incremental instances in time. (2) The reconstruction of the objects surface at these discrete time steps are stored into a reference animation A as surface states $S_0, S_1, ..., S_n$. (3) These discrete states are then used to generate temporally aligned displacement fields $D = \{d_1, d_2, ..., d_{n-1}\}$. These displacement fields are obtained using the non-rigid Coherent Point Drift (CPD) algorithm [9] between each set of consecutive surface states S_i, S_j. This allows us to identify topological correspondence regions as the topology of the reconstructed surface varies over time. (4) The optimization of both the geometric and material properties of the simulated object are obtained using the following formulation: $P(q, v, y, p)$ where (q) is the tetrahedral quality, (v) is the maximal tetrahedral volume (density coefficient), (y) is Young's Modulous and (p) is Possion's Ratio. (5) Based on the instance of the simulation mesh

defined by $P(q, v, y, p)$, we then optimize the forces inferred by the displacement fields to reconstruct the recorded animation of the form: $P(f, q, v, y, p)$ (Fig. 2).

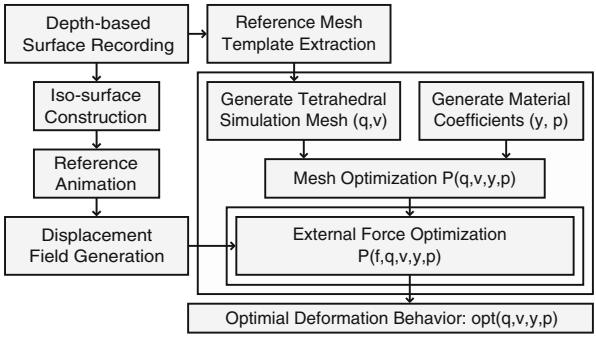

Fig. 2. Implemented methodology for the reconstruction of a surface-based recorded animation using simultaneous geometric and material parameter optimization. The enclosed regions illustrate the optimization hierarchy.

This process is defined as a compound non-linear optimization that identifies the optimal forces to apply to the deformable mesh in each simulation time-step for each unique parameterization of the geometric construction and elastic material parameters of the model. The objective function of this optimization process is to minimize the displacements generated between the simulated surface and the scanned reference animation during each simulation time-step. The output of this approach is the set of geometric and material parameters $opt(q, v, y, p)$ that can be used with the set of optimal external forces f for each simulation time-step to accurately reconstruct the recorded deformation.

4 Deformable Surface Tracking

The process of recording the behaviors of a deformable object's surface state has been well explored [10,11] and approaches using high-speed video as well as and depth-based surface scanning techniques [12] have begun to emerge as a large segment within the field of elastic material property extraction. In our approach, we can utilize the improved sampling rates of modern depth-imaging devices to capture the deformation behaviors of real-world objects in real-time.

As a prerequisite for our optimization procedure, we assume that the surface of the deforming object can be acquired through a sequence of depth-images or point-clouds that can be obtained using synchronized depth-imaging devices. These scans are then automatically aligned using existing techniques [13–15] to form an accurate approximation of the deforming object's surface over time. We define this sequence of aligned depth images as the input of one animation frame within A, which will be used to represent the topology of the recorded object.

Our approach assumes the point-cloud representing the objects entire surface at each discrete time increment is defined as a set of unordered point set with estimated surface normals [16]. To reduce the density of the provided point clouds we employ a simple standard-deviation outlier filter and voxel-based reduction filters provided within PCL [17]. Point-cloud segmentation for background removal is beyond the scope of this work and is handled in a pre-processing stage.

5 Surface Animation Reconstruction

The process of establishing a reference animation that defines the deformation behavior of the recorded object over time is defined as a set of surface states that are reconstructed by each discrete surface point-cloud into a set of n frames to generate the reference animation A. For each scanned surface state $S_i \in A$ containing an oriented point set, we employ the volumetric iso-surface reconstruction algorithm presented in [18] to reconstruct the surface of the object in each recorded frame. This algorithm takes the oriented point set in each state and utilizes a Marching Cubes (MC) [19] variant to extract a surface mesh that accurately represents the surface of the scanned object. Due to the high resolution of the resulting mesh that contains a large number of sliver triangles due to the MC surface extraction process, we utilize a filtering process to eliminate these defects and any degenerate triangles [20].

The result of this process is a high-quality discrete surface animation that describes the deformation behavior of the recoded object. We explicitly note the requirement of generating a high-quality mesh for the objects rest-state. Due to our template-free approach, we extract the simulation surface from the surface state S_0 to generate the tetrahedral mesh used in our simulation optimization. An example of the input surface point clouds and their corresponding surface reconstructions are illustrated in Fig. 3. This allows us to automatically generate the physical representation of our simulation mesh which is required for the process of optimizing the internal geometry of the recorded object.

6 Rest-State Mesh Generation

The basis of our automated optimization process relies on the ability to extract a high quality tetrahedral mesh from the first frame of the reference animation

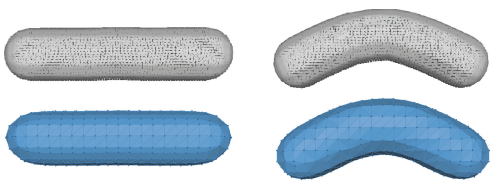

Fig. 3. Surface reconstruction of two scanned surface states: the input surface point-clouds (top) and their corresponding surface reconstructions (bottom) define the reference surface animation A.

A. This tetrahedral mesh represents the geometric construction of the mesh used within the simulation to reconstruct the observed deformation behavior. Ensuring that the quality of the surface state $S_0 \in A$ allows us to provide a reliable procedural regeneration process for creating a high quality simulation mesh. Based on the triangulated surface provided by the iso-surface extraction algorithm, we employ the Delaunay-based tetrahedral construction algorithm implemented within Tetgen [21]. The images in Fig. 4 illustrate the change in distribution and density of the tetrahedral components that compose the internal geometry of the simulated object. The quality and density of the generated tetrahedra are varied based on the parametrization $P(q, v)$. The images in Fig. 4(a) illustrate the slight difference in geometric density that contribute to a different deformation characteristic and the comparison presented in Fig. 4(b) illustrates a slight variance in the tetrahedral quality leading to elongated tetrahedral components.

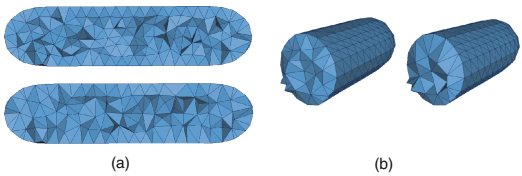

Fig. 4. Tetgen generated tetrahedral mesh based on the surface state S_0. The images in (a) and (b) illustrate two different potential geometric densities generation during the optimization process.

The quality of a tetrahedral element within the simulation mesh is defined as the radius-edge ratio of the generated tetrahedra. The objective of this parameter is to ensure that a minimal number of sliver tetrahedra (those with excessively small or large dihedral angles) are introduced into the internal structure of the object. These forms can introduce unwanted artifacts within the surface of the deforming object and alter the distribution of the homogeneous material we aim to model. Similarly the restriction of the maximal tetrahedral volume alters the observed deformation behavior of the object under a constant set of external forces. The density of the geometric structure defined by this parameter impacts the magnitude of the external forces applied to reach the desired deformation.

7 Deformation Force Optimization

The collection of surface states used to determine the displacements of the deformation behavior of the object are also used to generate the required external forces that imposed the deformation. Since our approach assumes that no information about the external forces imposed on the reference object, we present an automated method of estimating these forces using the displacement fields generated from the discrete differences in the input surface sequence defined within the generated reference animation.

Based on the surface displacement exhibited by the scanned object between discrete states within the reference animation, we form the generated external forces by calculating an approximate linear velocity and acceleration of the surface. This pseudo acceleration is defined through the linearization of the displacement given the discrete time-step dt. From this we derive the linear velocity $v = d_i/dt$ and pseudo acceleration $\alpha = dv/dt$ where the mass coefficient for each discrete surface node is one and the external force is defined as $\mathscr{F} = m\alpha$.

The error metric presented in the objective function of this optimization is based on the magnitude of the displacement field generated between the current simulation mesh surface consisting of p_n points and the alignment of these points to the scanned surface using the CPD algorithm. Equation 1 defines the objective function as the norm of the displacement field for this set of points between their current position and their resulting alignment with the next deformation surface state S_{i+1}.

$$|D| = \sum_{i=1}^{n} \| \, align(\boldsymbol{p}_i, S_{i+1}) - \boldsymbol{p}_i \| \tag{1}$$

Scanned surface reconstructions typically contain artifacts due to the depth measurement error associated with the employed depth-imaging device. Therefore rather than optimizing the simulated surface to match exact the topology changes and potential artifacts in the scanned surface within some tolerance, our approach generates the forces required to emulate the generalized deformation behavior to avoid artifacts. Using this approach we impose an approximation of the overall deformation behavior while maintaining physically plausibility.

8 Deformation Optimization

The optimization process that we utilize to derive the optimal deformation behavior of the simulated tetrahedral mesh with respect to the reference animation is composed of a two-phase process: (1) the geometric construction of the simulated object is generated using the current geometric parameters for tetrahedral quality and maximal tetrahedral volume along with the elastic material coefficients. (2) The forces required to achieve the deformation behavior observed in the reference animation are optimized with respect to this current parameterization as introduced in Sect. 7. This optimization is performed with a derivative-free optimization: Constrained Optimization by Linear Approximations [22] implemented within the NLopt numerical library [23].

As the elastic material properties and geometric construction of the tetrahedral mesh are updated, the new external forces required to impose the same deformation behaviors are naturally addressed through this optimization hierarchy. The objective of this non-linear optimization is to obtain the parameterization that provides the closest matching deformation behavior observed in the reference animation. This optimization is driven by the minimization between the simulated mesh surface with respect to the scanned surface state. From this

Table 1. Optimization parameterization $P(q, v, y, p)$ to generate the optimal deformation defined within the provided set of surface states $S_0, S_1, ..., S_n$.

Optimization parameter	q	v	y	p	$\|D_{anim}\|$
Geometric Opt $\|D_{anim}\|_{max}$	2.13242	1.01930e-4	1.000e6	0.300000	72.2366
Geometric Opt $\|D_{anim}\|_{opt}$	2.12500	1.01321e-4	1.000e6	0.300000	53.0002
Material Opt $\|D_{anim}\|_{max}$	2.00000	1.00000e-4	5.000e5	0.287500	75.4573
Material Opt $\|D_{anim}\|_{opt}$	2.00000	1.00000e-4	4.634e5	0.221214	53.3687
Geo + Mat $\|D_{anim}\|_{max}$	2.13601	8.01578e-5	6.55411e5	0.294876	75.7081
Geo + Mat $\|D_{anim}\|_{opt}$	2.12799	8.03421e-5	6.52945e5	0.297177	51.6883

metric we define the total deformation error of a given animation A as the sum of norms for each displacement field generated between the simulated surface and the scanned surface state as defined in Eq. 2.

$$|D_{anim}| = \sum_{S_i \in A} \sum_{j=1}^{n} \| \, align(\boldsymbol{p}_j, S_i) - \boldsymbol{p}_j \| \tag{2}$$

In this approach, we identify three configurations of this optimization process that illustrate the complex relationship between the geometric composition of the object, the elastic material properties, and the forces required to impose the recorded deformation. We formulate these configurations as follows: (1) Geometric optimization of the parameters $P(q, v)$ with the associated force optimization required to impose the recorded deformation. (2) The optimization of the FEM-based material parameters $P(y, p)$ with associated force optimization. The internal geometric composition of the object in this case is based on the optimal quality parameters defined by Tetgen ($q = 2.0$, $v = 1.0$). (3) The last configuration performs a complete optimization of the parameterization $P(q, v, y, p)$ to obtain the optimal uniform internal geometric structure and material properties required to match the recorded behavior.

9 Results

The results of our proposed simulation framework are illustrated through a synthetic deformation example of a scanned surface that represents a bend deformation imposed on a deformable object composed of a isotropic, homogeneous, elastic material. This object is scanned during the deformation process to capture the imposed deformation and our implementation extracts the external forces, geometric construction and elastic material properties through the optimization $P(f, q, v, y, p)$ to reproduce a simulation that matches the reference animation (Fig. 5).

The parameters provided in Table 1 define the parameterization of this optimization based on three configurations (1) optimizing only the internal geometric

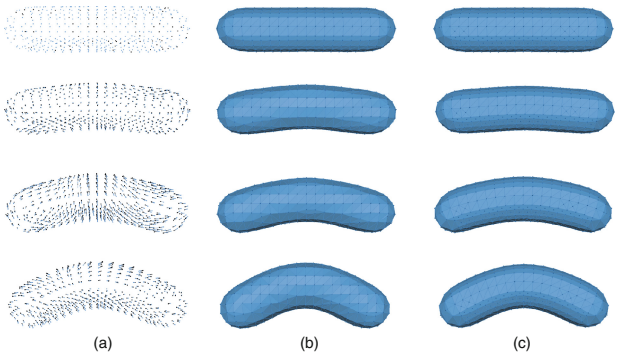

Fig. 5. Resulting deformation imposed on the simulated tetrahedral mesh based on the scanned deformation behavior. The image sequence displays the displacement fields of the observed deformation (a), the reconstructed scan surface over time (b), and the resulting simulated deformation (c).

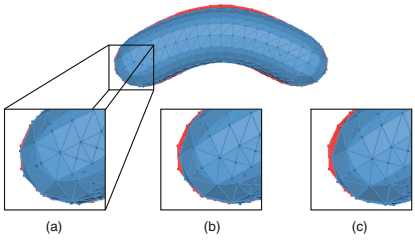

Fig. 6. Resulting alignment of the optimal parameterization (a) of the FEM mesh superimposed onto the scanned surface. The Geometric Opt (b) and Material Opt (c) results illustrate the misalignment obtained during the independent optimizations.

structure of the object with optimized external forces, (2) Fixing the ideal internal tetrahedral quality and density and optimizing only the material parameters, and (3) the process of optimizing all parameters of the form: $P(q, v, y, p)$.

The results provided through our optimization process indicates that simultaneously optimizing the external forces with respect to the internal geometric structure $P(q, v)$ and the elastic material properties of the FEM-based model $P(y, p)$ provides a closer approximation of the input animation A. Based on the set of external forces estimated from the displacement fields generated from the input surface states, we illustrate the complex relationship between the applied forces, geometric structure, and material properties exacerbate the difficulty in extracting an exact deformation replication. This is indicated by the slight numerical adjustments that made to the optimization parameters provided in Table 1 drastically alter the resulting animation displacement score $|D_{anim}|$. The result in Fig. 6 provides the optimized superimposed alignment between the

simulated mesh and the scanned surface, illustrating the improvement obtained through optimizing both geometric composition and elastic material properties.

10 Evaluation

The core of our methodology provides an accurate behavioral alignment however, it relies on the ability to extract the physical model from the reference frame S_0 within the animation A. For complex geometric structures there are instances where surface occlusions will degrade the quality of the generated surface. These occlusions can not only reduce the quality of the simulation mesh but also interfere with the recorded deformation behavior.

The process of optimizing the forces required to drive the deformation behavior defined by the subsequent displacement fields generated from the original surface animation can introduce drift between the simulated FEM model and the recorded surface. This can introduce an unintended translation and net torque to be imposed during the force optimization process. Due to the generalized nature of the external forces generated in our approach, exact surface deformations may not be obtained. While our technique avoids the propagation of any imperfections in the scanned surface through the generalized deformation behavior, we still may not obtain an exact replica of the observed deformation. However this process can be directed towards reproducing physically plausible deformation behaviors based on a guided reference model.

11 Conclusion

In this work we have present an automated methodology for extracting the deformation behavior for a scanned surface of an object composed of a homogeneous elastic material that exhibits isotropic characteristics. We present an effective method for extracting a quality tetrahedral simulation mesh from an input scanned surface and illustrated the behavioral impact of optimizing both the geometric structure and material properties with respect to a set of unknown external forces. Based on the implementation of our approach, our method was able to generate a high-quality animated surface sequence, procedurally generate the physical representation of the object, derive the eternal forces and optimal material properties required to impose the deformation observed in the scanned surface. Furthermore, our method validates the process of simultaneously optimizing the geometric construction of the simulated object with the FEM-based elastic material properties to improve the deformation generated in the force optimization process, thus providing an objective analysis of our displacement-driven simulation and illustrating the impact of geometric density with FEM-based simulations.

References

1. Wuhrer, S., Lang, J., Tekieh, M., Shu, C.: Finite element based tracking of deforming surfaces. Graph. Mod. **77**, 1–17 (2015)

2. Choi, J., Szymczak, A.: Fitting solid meshes to animated surfaces using linear elasticity. ACM Trans. Graph. **6**(1–6), 10 (2009)
3. Barbic, J.: Vega fem library. A physics library for three-dimensional deformable object simulation (2015). http://run.usc.edu/vega/
4. Becker, M., Teschner, M.: Robust and efficient estimation of elasticity parameters using the linear finite element method. In: Schulze, T., Preim, B., Schumann, H. (eds.) SimVis. SCS Publishing House e.V., Erlangen (2007)
5. Frank, B., Schmedding, R., Stachniss, C., Teschner, M., Burgard, W.: Learning the elasticity parameters of deformable objects with a manipulation robot. In: IEEE/RSJ International Conference on Intelligent Robots and Systems, pp. 1877–1883 (2010)
6. Cagniart, C., Boyer, E., Ilic, S.: Iterative deformable surface tracking in multi-view setups. In: 5th International Symposium on 3D Data Processing, Visualization and Transmission, 3DPVT (2010)
7. Bianchi, G., Solenthaler, B., Szekely, G., Harders, M.: Simultaneous topology and stiffness identification for mass-spring models based on fem reference deformations. In: Medical Image Computing and Comptuer-Assisted Intervention (2004)
8. Furukawa, Y., Ponce, J.: Dense 3d motion capture from synchronized video streams. In: IEEE Conference on Computer Vision and Pattern Recognition (2008)
9. Myronenko, A.: Point-set registration: coherent point drift. IEEE Trans. Pattern Analy. Mach. Intell. **32**, 2262–2275 (2010)
10. Schulman, J., Lee, A., Ho, J., Abbeel, P.: Tracking deformable objects with point clouds. In: International Conference on Robotics and Automation (2013)
11. Hur, J., Lim, H., Ahn, S.C.: 3D deformable spatial pyramid for dense 3D motion flow of deformable object. In: Bebis, G., Boyle, R., Parvin, B., Koracin, D., McMahan, R., Jerald, J., Zhang, H., Drucker, S.M., Kambhamettu, C., El Choubassi, M., Deng, Z., Carlson, M. (eds.) ISVC 2014, Part I. LNCS, vol. 8887, pp. 118–127. Springer, Heidelberg (2014)
12. Li, Y., Chen, C.F., Allen, P.K.: Recognition of deformable object category and pose. In: International Conference on Robotics and Automation (2014)
13. Chen, Y., Medioni, G.: Object modeling by registration of multiple range images. In: Proceedings of IEEE International Conference on Robotics and Automation, vol. 3, pp. 2724–2729 (1991)
14. Besl, P., McKay, N.D.: A method for registration of 3-d shapes. IEEE Trans. Pattern Anal. Mach. Intell. **14**(2), 239–256 (1992)
15. Rusu, R., Blodow, N., Beetz, M.: Fast point feature histograms (fpfh) for 3d registration. In: IEEE International Conference on Robotics and Automation, ICRA 2009, pp. 3212–3217 (2009)
16. Rusu, R.B.: Semantic 3D Object Maps for Everyday Manipulation in Human Living Environments Ph.D. thesis, Computer Science, Universitaet Muenchen, Germany (2009)
17. Source, O.: Pcl: the point cloud library is a standalone, large scale, open project for 2d/3d image and point cloud processing (2015). http://pointclouds.org/
18. Kazhdan, M.: Reconstruction of solid models from oriented point sets. In: Proceedings of the Third Eurographics Symposium on Geometry Processing, SGP 2005, Eurographics Association (2005)
19. Lorensen, W.E., Cline, H.E.: Marching cubes: a high resolution 3d surface construction algorithm. In: Proceedings of the 14th Annual Conference on Computer Graphics and Interactive Techniques, SIGGRAPH 1987, pp. 163–169. ACM (1987)
20. Curless, B., Levoy, M.: A volumetric method for building complex models from range images. In: Proceedings of SIGGRAPH 1996, pp. 303–312 (1996)

21. Si, H.: TetGen: a quality tetrahedral mesh generator and three-dimensional delaunay triangulator (2007). http://wias-berlin.de/software/tetgen/
22. Powell, M.: A direct search optimization method that models the objective and constraint functions by linear interpolation. In: Gomez, S., Hennart, J.-P. (eds.) Advances in Optimization and Numerical Analysis. Mathematics and Its Applications, vol. 275, pp. 51–67. Springer, Heidelberg (1994)
23. Johnson, S.G.: Nlopt: the nlopt nonlinear-optimization package (2015). http://ab-initio.mit.edu/nlopt